Chapter 6

ISOTHERMAL HOT CORROSION BEHAVIOR OF SUPER AUSTENITIC STAINLESS STEEL 904L IN AIR AT 500-650 ˚C

Chapter 6

ISOTHERMAL HOT CORROSION BEHAVIOR OF SUPER AUSTENITIC STAINLESS STEEL 904L IN AIR AT 500-650 ˚C

6.1. INTRODUCTION

Several investigations have been carried out in the past on hot corrosion of various metallic materials, designed for high temperature application such as several grades of boiler tubes, by alkali sulphates and different chlorides [105-109]. Neilsen et al. [110] explored implications of corrosion associated with chlorine on the operation of Biomass fired boilers and found that alkali chloride salts in deposits can cause fast corrosion, even below the melting points of salts. Enestam et al. [23] compared corrosiveness of NaCl and KCl on super heater tubes of steam boilers and found that both were equally corrosive in the temperature range of 400-650 ˚C. Liu et al. [22], studied hot corrosion behavior of boiler tube alloys in waste to energy plants and observed that the corrosivity was lowest from the $CaCl_2$ and highest from $FeCl_2$. Further, degradation of the materials T22, Esthete 1250 and Sanicro 28, at 500 ˚C was comparable at 500 ˚C during short exposure, however, on long exposure of 1000 h there was variation in thickness of the corroded layer on these alloys. Among the deposits, KCl is the main content which corroded the low alloy steels of bolier tube material, at much faster rate at as low as 400 ˚C [87], and stainless steel at 550 ˚C [40].

This chapter presents isothermal hot corrosion behavior of 904L super austenitic stainless steel in the salt mixtures of alkali sulphates and chlorides at 500, 550, 600 and 650 °C for time durations of 25, 50, 75, and 100 h in still air. The details of experimental procedures are given in the section 2.3 of Chapter 2.

6.2. RESULTS

6.2.1 CORROSION KINETICS

The weight gain per unit area (ΔW) versus time (t) plots of the samples coated with SM1 and SM2 and isothermally exposed at 500-650 ˚C for the durations of 25, 50, 75 and 100 h are shown in **Figures 6.1 and 6.2** respectively. It is evident from the **Figures 6.1a and 6.2a** that there is progressive increase in ΔW with the duration and the temperature of exposure. The weight gain is lowest at 500 ˚C and highest at 650 ˚C. It may be seen from the much smaller scale of ΔW in **Figure 6.1a** that in the samples coated with SM1, there is much slower and steady increase in ΔW from the exposure of 0-100 h in comparison with that in the samples coated with SM2 (**Figure 6.2a**) at the temperatures of exposure from 500-650 ˚C.

It may be seen from slopes of ΔW *vs* t plots in **Figures 6.1** and **6.2** that the rate of weight gain is fast during the initial period of 25 h of exposure, thereafter the slope of the curve continuously decreases. The kinetics of the process of hot corrosion was analysed from the relationship given in equation 3.1 of Chapter 3.

The value of the parabolic rate constant (k_p) is found to increase with increase in temperature from 500-650 ˚C. The plots of $(\Delta W)^2$ *vs.* t for the samples coated with SM1 and SM2 are shown in Figures 6.1a and 6.2b respectively. From straight-line nature of these plots, it is obvious that near parabolic behavior is exhibited. The values of the parabolic rate constant kp for the SM1 and SM2 coated samples are presented in **Table 6.1**.

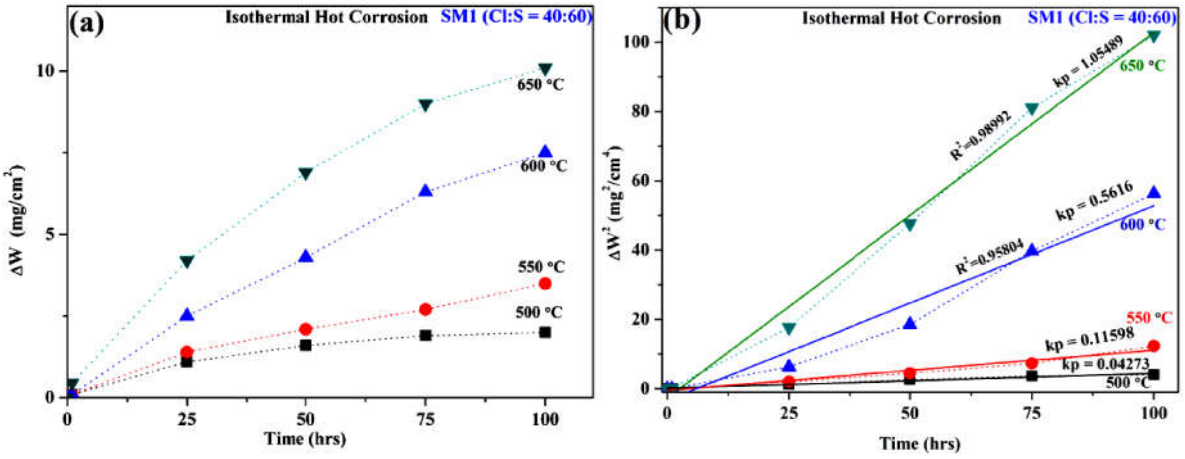

Figure 6.1: Plots showing corrosion behavior of SASS 904L coated by SM1, during isothermal exposure at 500-650 °C from 25-100 h: (a)(ΔW) vs time and (b))(ΔW)^2 vs time.

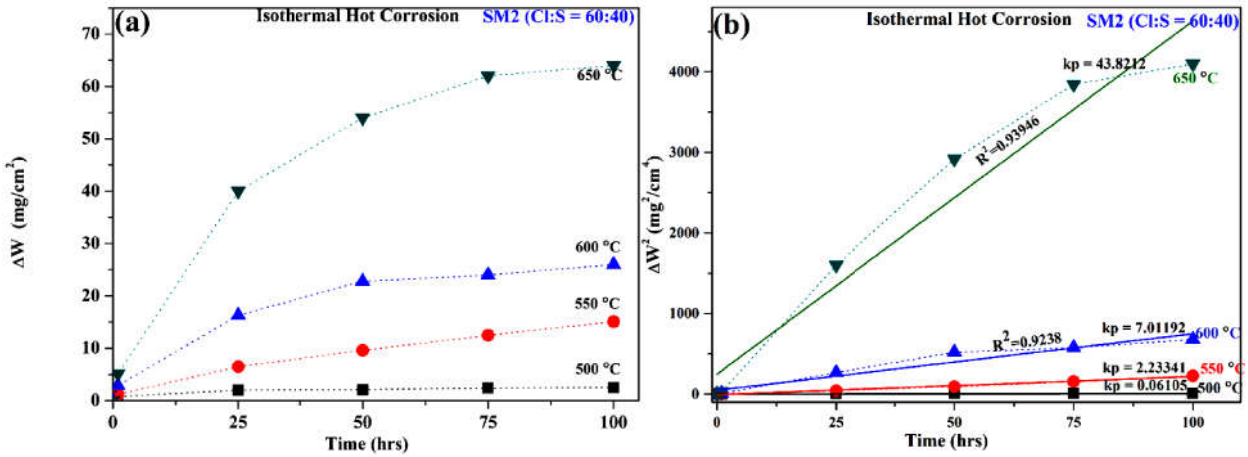

Figure 6.2: Plots showing corrosion behavior of SASS 904L coated by SM2, during isothermal exposure at 500-650 °C from 25-100 h: (a)(ΔW) vs time and (b))(ΔW)^2 vs time.

Table 6.1: Weight gain per unit area (ΔW) and kinetic rate values of isothermally exposed samples at 500-650 ˚C, from 25-100 h under SM1 and SM2 salt coated environment.

Temperature (˚C)	Salt Mixture	ΔW (mg)	Time (h)	k_p(mg^2·cm^{-4}·h^{-1})	R^2
500	SM1	2	0-100	0.043	0.97038
	SM2	2.5	0-100	0.061	0.90001
550	SM1	3.5	0-100	0.116	0.96141
	SM2	15.1	0-100	2.233	0.98674
600	SM1	7.5	0-100	0.562	0.95804
	SM2	26	0-100	7.012	0.9238
650	SM1	10.1	0-100	0.17	0.98992
	SM2	64	0-100	43.821	0.93946

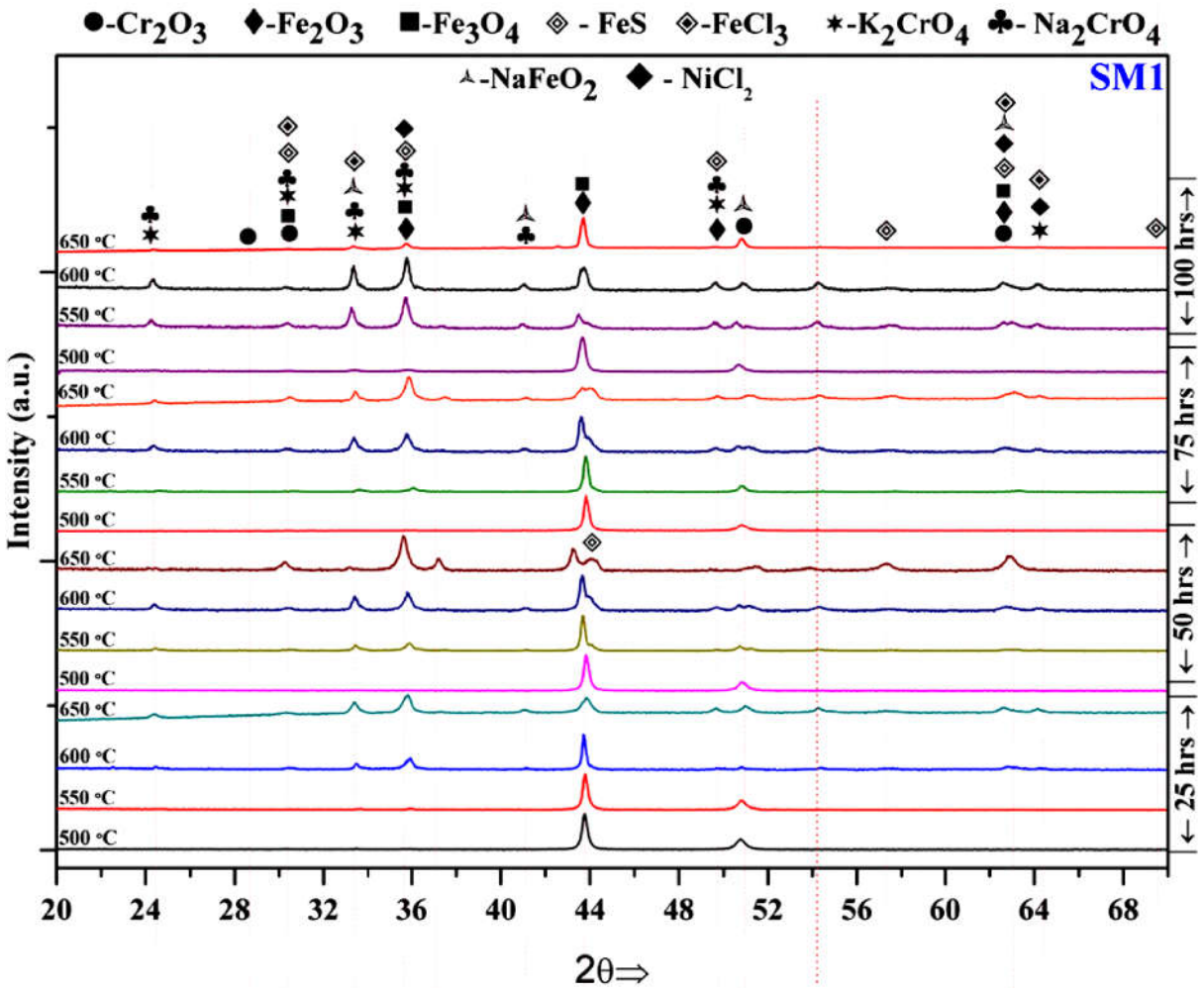

Figure 6.3: Phase analysis of the SM1 coated samples, isothermally exposed at 500-650 ˚C for 25-100 h.

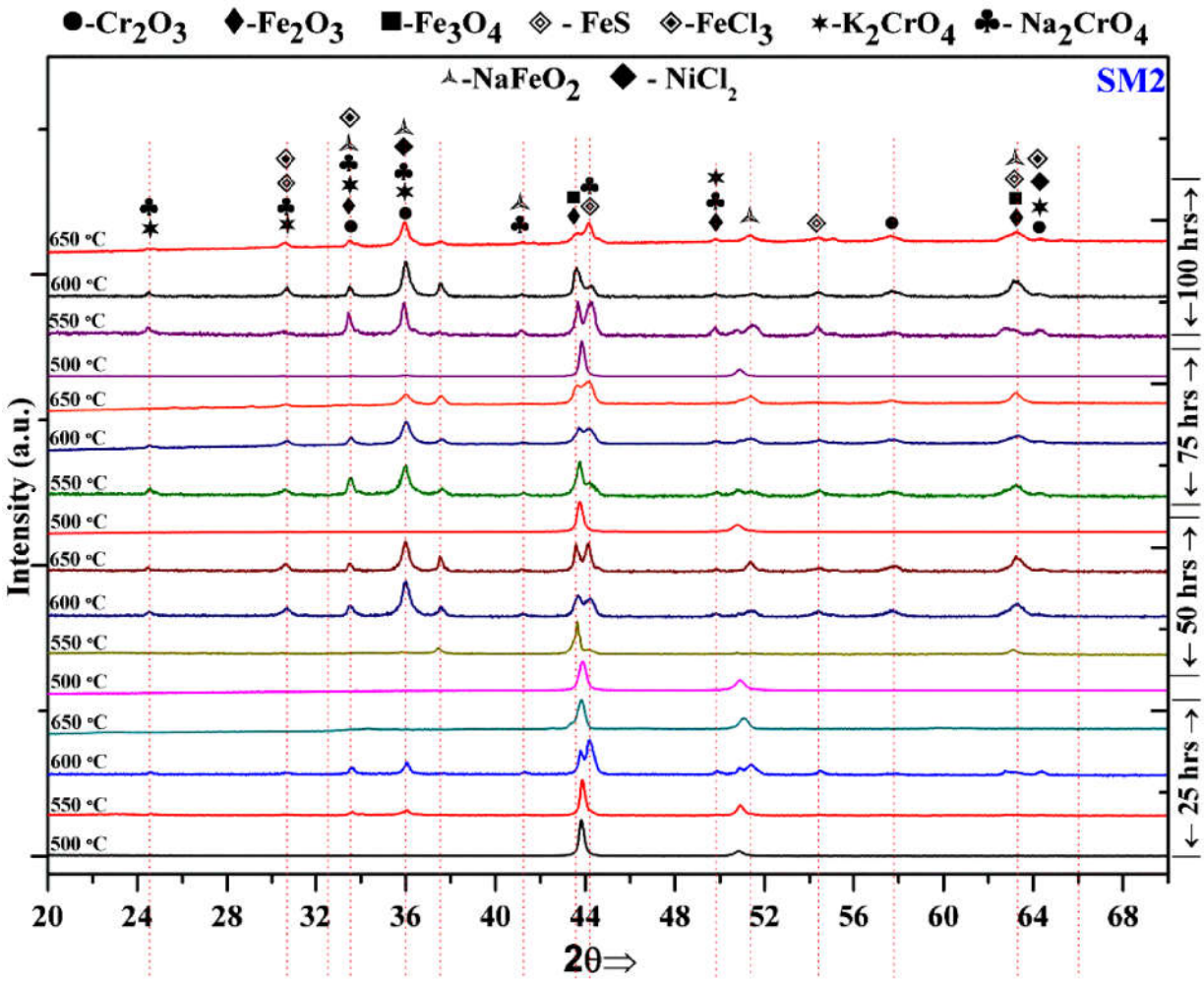

Figure 6.4: Phase analysis of the SM2 coated samples, isothermally exposed at 500-650 ˚C for 25-100 h.

6.2.2 ANALYSIS OF CORRODED PRODUCTS

Figures 6.3 and 6.4 show XRD patterns of the corrosion products formed on the surface of the SM1 and SM2 coated samples respectively, exposed for 25-100 h at 500-650 ˚C. The various phases resulting from exposures of the SM1 and SM2 coated samples at different temperatures and for different durations are presented in **Table 6.2**. It may be seen from **Table 6.2** that there is presence of only iron oxide (Fe_2O_3/Fe_3O_4) in the SM1 and SM2

coated samples exposed at the lowest temperature of 500 ˚C even for the duration of 50 h whereas in the SM2 coated sample there is also presence of Cr_2O_3 along with Fe_2O_3/Fe_3O_4. In the SM1 coated sample there is presence of also Cr_2O_3 along with Fe_2O_3 and Fe_3O_4 but from the longer duration of 75 and 100 h at 500 ˚C. However, the number of phases increases with increase in the duration and temperature of exposure in both SM1 as well as SM2 coated samples.

Table 6.2: Phases formed after isothermal exposure of the SASS 904L at 500-650 ˚C from 25-100 h, in SM1 and SM2 coated environment.

Time (h)	Temp. (˚C)	Salt Mixture	
		SM1	**SM2**
25	500 ˚C	Fe_2O_3, Fe_3O_4	Fe_2O_3, Fe_3O_4
	550 ˚C	Cr_2O_3, Fe_2O_3, Fe_3O_4	FeS, Cr_2O_3, Fe_2O_3, Fe_3O_4, $KCrO_2$, $NaCrO_2$, $NaFeO_2$
	600 ˚C	Cr_2O_3, Fe_2O_3, Fe_3O_4, $KCrO_2$, $NaCrO_2$,	
	650 ˚C	Cr_2O_3, Fe_2O_3, Fe_3O_4, $KCrO_2$, $NaCrO_2$, $NaFeO_2$	
50	500 ˚C	Fe_2O_3, Fe_3O_4	Cr_2O_3, Fe_2O_3, Fe_3O_4
	550 ˚C	Cr_2O_3, Fe_2O_3, Fe_3O_4	FeS, Cr_2O_3, Fe_2O_3, Fe_3O_4, $KCrO_2$, $NaCrO_2$
	600 ˚C	Cr_2O_3, Fe_2O_3, Fe_3O_4, $KCrO_2$, $NaCrO_2$,	FeS, Cr_2O_3, Fe_2O_3, Fe_3O_4, $KCrO_2$, $NaCrO_2$, $NaFeO_2$
	650 ˚C	Cr_2O_3, Fe_2O_3, Fe_3O_4, $KCrO_2$, $NaCrO_2$, $NaFeO_2$	
75	500 ˚C	Cr_2O_3, Fe_2O_3, Fe_3O_4	Cr_2O_3, Fe_2O_3, Fe_3O_4, $KCrO_2$, $NaCrO_2$,
	550 ˚C	Cr_2O_3, Fe_2O_3, Fe_3O_4, $KCrO_2$, $NaCrO_2$	Cr_2O_3, Fe_2O_3, Fe_3O_4, $KCrO_2$, $NaCrO_2$, $NaFeO_2$
	600 ˚C	Cr_2O_3, Fe_2O_3, Fe_3O_4, $KCrO_2$, $NaCrO_2$, $NaFeO_2$	FeS, Cr_2O_3, Fe_2O_3, Fe_3O_4, $KCrO_2$, $NaCrO_2$, $NaFeO_2$
	650 ˚C		
100	500 ˚C	Cr_2O_3, Fe_2O_3, Fe_3O_4	Cr_2O_3, Fe_2O_3, Fe_3O_4, $KCrO_2$, $NaCrO_2$,
	550 ˚C	Cr_2O_3, Fe_2O_3, Fe_3O_4, FeS, $KCrO_2$, $NaCrO_2$, $NaFeO_2$	FeS, Cr_2O_3, $NiCl_2$, Fe_2O_3, Fe_3O_4, $KCrO_2$, $NaCrO_2$, $NaFeO_2$, K_2CrO_4,
	600 ˚C	Cr_2O_3, Fe_2O_3, Fe_3O_4, FeS, $KCrO_2$, $NaCrO_2$, $NaFeO_2$, Na_2CrO_4	
	650 ˚C	Cr_2O_3, Fe_2O_3, Fe_3O_4, FeS, NiCl2, $KCrO_2$, $NaCrO_2$, Na_2CrO_4	

6.2.3 MORPHOLOGY OF CORRODED SUARFACE

The morphology of the surfaces corroded by SM1 and SM2 coatings are shown by secondary electron images in **Figures 6.5** to **6.8** for the specimens exposed at 500, 550, 600 and 650 ˚C respectively. The micrographs a, b, c, d show surface features of the SM1 coated samples exposed for 25, 50, 75 and 100 h while the micrograph e, f, g, h show surface morphology of the SM2 coated samples exposed for the same durations of 25, 50, 75 and 100 h. It may be seen from Figure 6.5a that there is little effect of exposure on surface morphology of the SM1 coated sample exposed at 500 ˚C for 25 h whereas there is increase in the extent of corrosion, revealed from the surface morphology, with the duration of exposures (**Figures 6.5b,c,** and **d**). Globular features have developed in **Figures 6.5(b,c and d)**. Also, there is cracking of the surface features in some regions in **Figure 6.5d**. It is evident from the Table below **Figure 6.5** that there is little change in concentration of the different elements and oxygen content is low, in the enclosed region of **Figure 6.5a**. On the other hand, there is decrease in chromium content and more so in nickel and iron content and sufficient increase in the oxygen content. Further, there is increase in the concentration of potassium and chlorine. There is variation in concentration of the different elements from one to other enclosed regions in **Figure 6.5c-d**. The surface morphologies of the specimens coated by SM2 and exposed at 500 ˚C are quite different from that of the SM1 coated specimens exposed at 500 ˚C. The corrosion affected region in **Figure 6.5e** is relatively more than that in **Figure 6.5a** and there are pores of varying sizes on the corroded surface. There is increase in the corroded region in **Figure 6.5f** than that in **6.5e**. There are very small globular features on the surface along with pores in some regions. There is exfoliation of blister like features in **Figure 6.5g**. There is formation of

nodules covered with fine globules and also distinct cracking of the surface layer in **Figure 6.5h**. There is decrease in chromium content and nickel content whereas increase in iron content (**Figure 6.5f-g**).

The surface morphology of the samples exposed at 550 ˚C for different durations of exposure, coated by SM1 and SM2 are shown in **Figure 6.6(a,b,c,d)** and **Figure 6.6(e,f,g,h)** respectively. It may be seen that area fraction of the corroded region of the sample exposed for 25 h (**Figure 6.6a**) is larger than of that exposed at 500 ˚C for the same duration of exposure (**Figure 6.5a**). There is exfoliation and spalling of the scale in some regions (**Figure 6.6c**) and cracking of the scale (**Figure 6.6d**). In case of SM2 coated samples there is non-uniform corrosion and spallation of the scale from large area (**Figure 6.6h**). It may be seen from the table below **Figure 6.6** that there is decrease in chromium content with increase in the duration of exposure, relatively more in the SM2 coated samples. There is similar trend in content of nickel. On the other hand oxygen content is nearly comparable in SM1 and SM2 coated samples. **Figure 6.7** displays surface morphologies of the samples coated with SM1 (**Figure 6.7a,b,c,d**) and SM2 (**Figure 6.7e,f,g,h**) exposed at 650 ˚C for 25, 50,75 and 100 h. The area fraction of corroded region at 600 ˚C of the SM1 coated sample exposed at 600 ˚C (**Figure 6.7a**) is larger than of those exposed at lower temperatures (**Figures 6.5a** and **6.6a**). There is increasing tendency of development of globular features with increase in the duration of exposure (**Figure 6.7b,c,d**) and also in cracking of the corroded layer. There is much larger extent of spallation of the corroded scale in the SM2 coated specimens, increasing with the duration of exposure from 25 to 100 h (**Figure 6.7e,h**). It is evident from the Table (below **Figure**

6.7) that contents of Chromium and iron are much higher in the spalled region (**Figure 6.7e,f,d**).

Figure 6.8 shows surface morphologies of the SM1 and SM2 coated samples exposed at 650 ˚C for varying durations from 25-100 h. There is spalling of the scale in both types of specimens coated with SM1 as well as SM2, increasing with the duration of exposure.

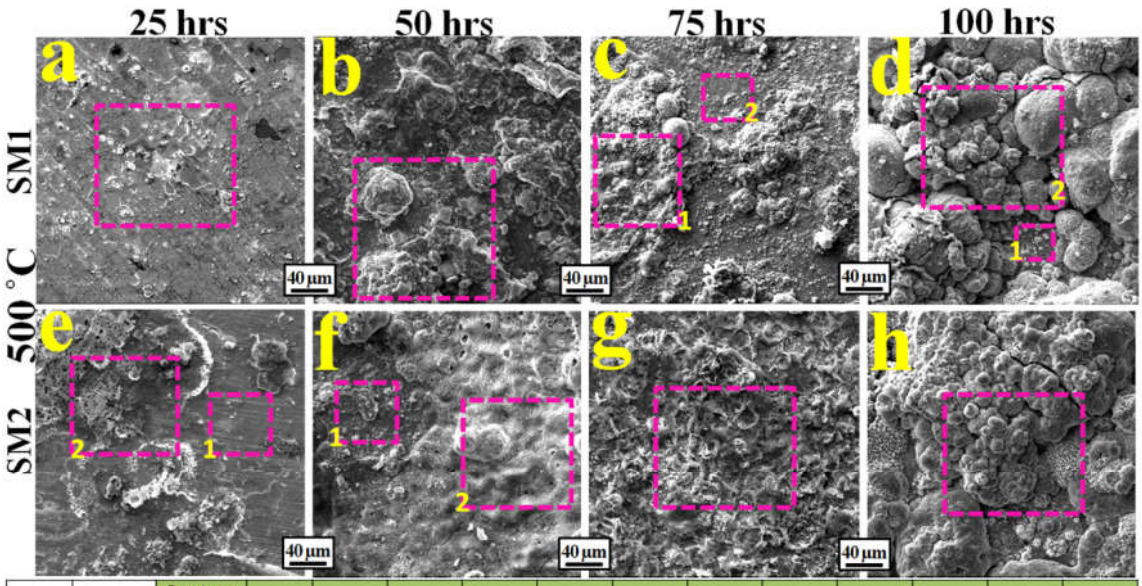

	Figure	Spectrum (wt%)	Mn	Mo	Cr	Ni	Fe	Si	Cu	O	Na	K	S	Cl
SM1	6.5a	1	1.01	1.20	16.54	27.79	36.83	0.38	1.36	14.13	0.21	0.24		0.02
	6.5b	1	1.40		15.77	1.50	3.77	1.10	0.56	40.56	12.78	9.25	7.82	5.03
	6.5c	1			12.70	13.44	38.69			29.21	2.63	0.86	1.10	1.37
		2	1.59	1.80	19.55	4.35	40.55		1.19	30.85				
	6.5d	1	1.20	1.69	18.94	6.98	38.87	0.14	0.18	31.39	0.14	0.11	0.02	0.03
		2	0.04	0.32	6.82	13.07	25.88		1.86	36.17	7.87	4.29	2.05	1.27
SM2	6.5e	1	1.28	1.79	16.39	28.96	35.77	0.20	0.13	13.71	0.45		0.79	0.51
		2	1.21	4.30	15.56	24.02	35.02	0.36	1.01	17.30	0.22	0.26	0.21	0.44
	6.5f	1	0.37		14.88	0.47	12.20		0.34	37.12	12.43	14.32	6.12	1.14
		2	1.21		10.63	4.23	44.70			27.83	4.78	1.23	2.28	2.73
	6.5g	1	0.92		11.16	6.78	47.07		0.71	30.08	1.45	1.01	0.11	0.68
	6.5h	1	11.93		10.87	5.45	28.12			33.26	3.52	4.04	2.35	0.37

Figure 6.5: Morphology and analysis of surface of the samples isothermally exposed at 500 ˚C: (a,b,c,d) coated with SM1 and (e,f,g,h) coated with SM2.

The severity of scale spallation is much higher in the SM2 coated samples, it is multi-layer (**Figure 6.8e,f,g,h**) whereas it is one layer spallation in the SM1 coated samples. There is much variation in contents of the different alloying elements in different regions of the scale.

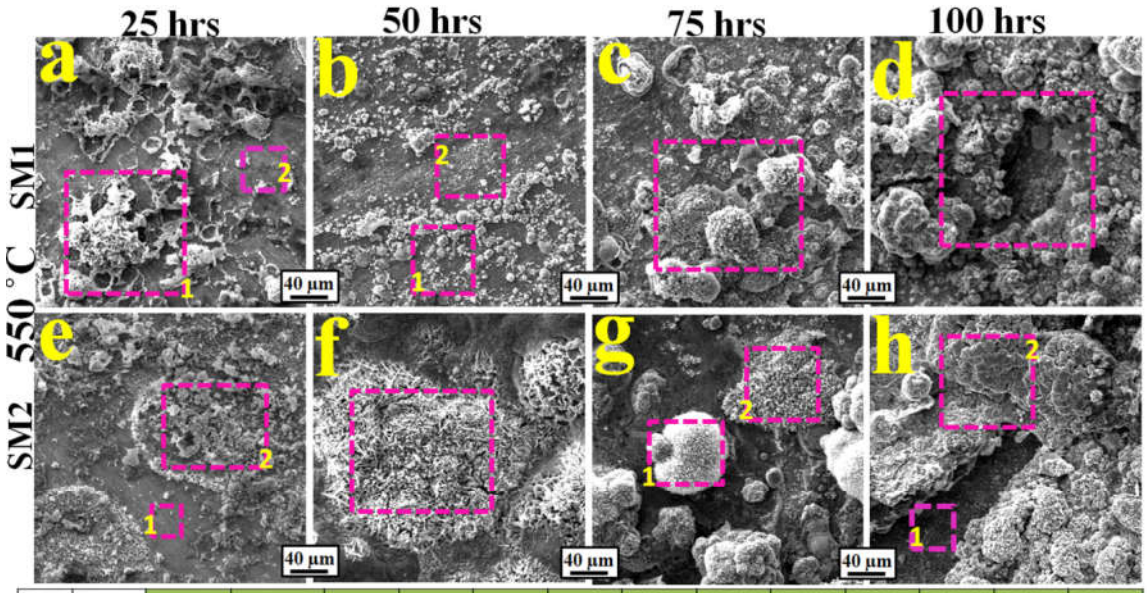

	Figure	Spectrum (wt%)	Mn	Mo	Cr	Ni	Fe	Si	Cu	O	Na	K	S	Cl
SM1	6.6a	1	1.11	1.56	15.31	19.45	36.11	0.15	1.04	22.50	0.58	0.17	1.20	0.81
		2	1.20	4.29	15.65	23.02	36.03	0.30	1.06	18.00	0.12	0.23	0.1	0.04
	6.6b	1	1.30	1.74	16.48	28.49	36.06	0.20	0.13	13.61	0.91		0.69	0.38
		2	0.42		18.71	7.31	40.17	0.18	0.41	32.23	0.01	0.01	0.02	0.01
	6.6c	1	3.13	1.53	6.68	2.95	58.73		0.65	24.91	0.51	0.45	0.14	0.19
	6.6d	1	2.89	0.52	8.67	6.92	49.10		3.08	27.06	0.21	0.58		
SM2	6.6e	1	2.51		8.27	5.50	58.94	0.25	0.97	21.56	0.62	0.09	0.84	0.38
		2	2.55		9.33	5.23	48.81	0.04		33.19		0.07	0.55	0.22
	6.6f	1	0.04		0.51	1.35	1.93	1.30	0.48	26.39	5.48	37.50	0.58	22.88
	6.6g	1	0.06	0.10	4.67	10.35	7.81	1.30	0.48	21.24	5.48	37.50	0.67	10.12
		2	2.73	0.02	3.13	3.36	55.40	0.01	2.94	28.63	1.40	0.86	1.01	0.04
	6.6h	1	2.38	0.05	2.34	0.39	63.69	0.13	0.71	30.22	0.01	0.04		
		2	12.84		3.08	3.56	48.37	0.59	2.70	28.85				

Figure 6.6: Morphology and analysis of surface of the samples isothermally exposed at 550 ˚C: (a,b,c,d) coated with SM1 and (e,f,g,h) coated with SM2.

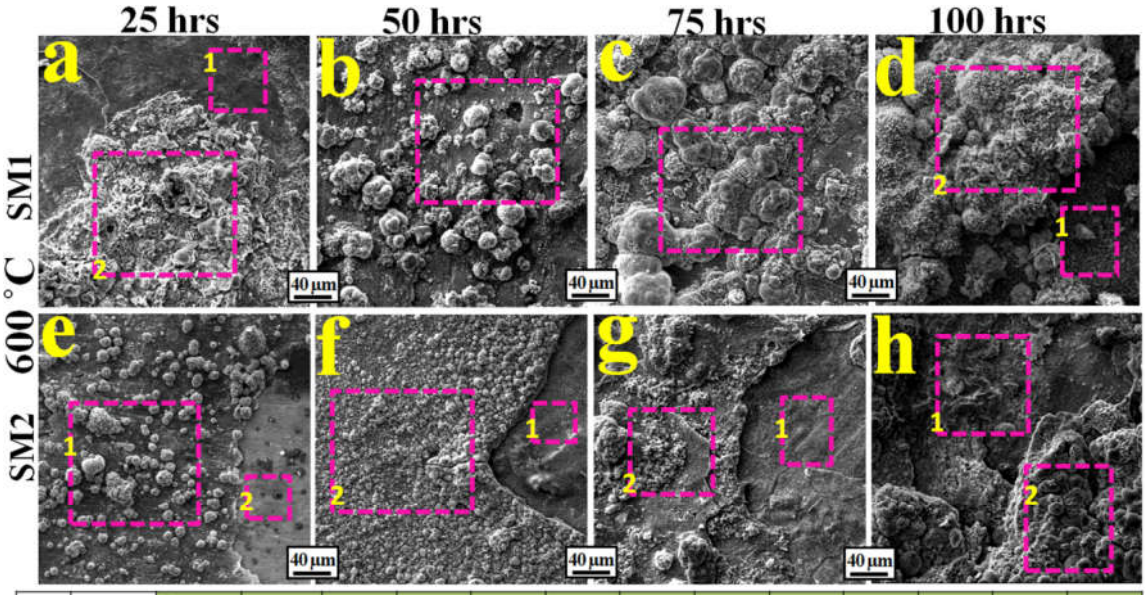

	Figure	Spectrum (wt%)	Mn	Mo	Cr	Ni	Fe	Si	Cu	O	Na	K	S	Cl
SM1	6.7a	1	0.30		12.74	40.04	17.02	1.13		28.07				
		2	3.08		5.64	3.64	46.49	0.14	4.67	34.94	0.41	0.34		
	6.7b	1	3.22		7.03	2.40	55.47	0.78	1.21	28.22	0.52	0.82	0.26	0.03
	6.7c	1	0.96	0.03	2.34	0.39	67.69	0.13	0.71	26.32	0.08	0.87	0.27	0.18
	6.7d	1	1.52	1.4	14.8	21.87	39	0.03	0.3	20.37	0.18	0.02	0.16	0.15
		2	2.74	0.61	5.02	1.97	59.12	0.19	0.83	28.50	0.21	0.40	0.19	0.16
SM2	6.7e	1	1.07	2.10	7.34	11.81	45.41	1.06	1.08	26.99	1.21	1.52	0.01	0.04
		2	1.62	2.40	18.21	16.45	37.15	0.55	1.20	20.76	0.18	0.31		
	6.7f	1	1.98	0.72	13.2	15.63	36.5	0.18	0.09	30.92	0.01	0.02	0.01	0.01
		2	0.31	1.51	9.64	32.94	27.35	1.62	0.63	25.97				
	6.7g	1	1.72	1.11	17.71	5.66	40.52	0.36	0.40	31.92				
		2	1.80	1.12	10.03	17.58	36.20	0.67	2.45	29.05	0.12	0.41	0.31	0.08
	6.7h	1	1.85	4.04	9.08	23.38	24.19	3.00	1.58	32.53	0.03	0.14	0.04	
		2	1.00	2.45	9.23	39.80	21.96	0.48		24.88				

Figure 6.7: Morphology and analysis of surface of the samples isothermally exposed at 600 ˚C: (a,b,c,d) coated with SM1 and (e,f,g,h) coated with SM2.

6.2.4 SEM CROSS-SECTION AND ELEMENTAL MAPPING

Cross-sections of the SM1 and SM2 coated samples isothermally exposed at 650 ˚C for 25 and 100 h are shown in **Figures 6.9** and **6.10** respectively. The interface of the substrate and the corroded scale is not intact in **Figure 6.9a**. Voids may be seen at the interface. Also, the scale is not smooth. The peaks of the different elements are shown in **Figure**

6.9b. It is evident from the elemental mapping that the concentration of oxygen is there in the central region. In the upper portion of the scale there is much less content of chromium, iron and nickel. Similarly, in the SM2 coated sample the scale is not intact with the substrate also the scale is quite uneven (**Figure 6.10a**). The peaks of the different elements are shown in **Figure 6.10b**. Oxygen enrichment is in larger region than that in the SM1 coated sample. There is depletion of iron, chromium and nickel to larger depth than that in the SM1 coated sample.

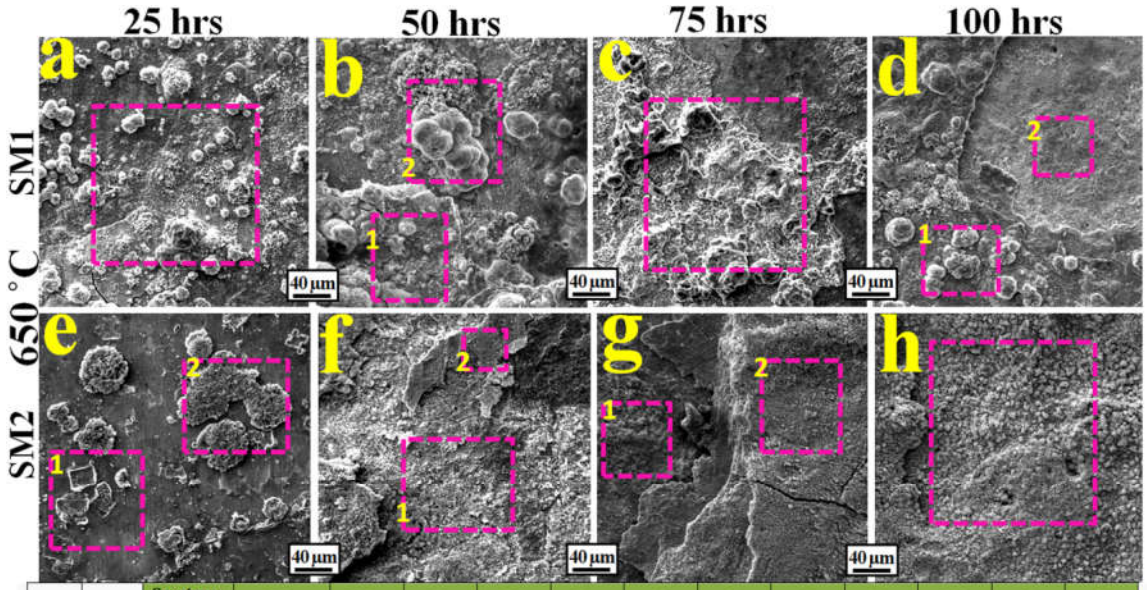

	Figure	Spectrum (wt%)	Mn	Mo	Cr	Ni	Fe	Si	Cu	O	Na	K	S	Cl
SM1	6.8a	1	2.75	0.59	4.11	4.53	54.26	0.23	3.10	27.43	1.01	0.61	0.12	0.45
	6.8b	1	1.65	0.39	1.30	0.96	64.91	2.03	0.25	27.49	0.03	0.43	0.20	
		2	1.29	2.42	7.27	12.19	41.21	1.36		34.27	0.03	0.07		
	6.8c	1	1.83	1.77	8.75	16.27	40.00		0.55	29.82	0.07	0.61	0.21	
	6.8d	1	0.15	14.49	4.22	53.92	15.51	0.87	1.12	7.09	1.16	0.08	1.38	
		2	2.06	0.15	4.64	0.51	68.78	0.07	0.82	22.67	0.15		0.04	0.10
SM2	6.8e	1	1.43	2.1	29.12	3	38.41			21.65	0.49	3.51		
		2	1.12	1.98	31.03	3.46	39.71			19.54	2.91	0.13		
	6.8f	1	2.04	3.71	10.96	30.19	25.23	0.81	0.62	25.52		0.44	0.37	0.11
		2	1.15	1.12	5.46	43.08	18.15	0.40	0.69	29.10	0.44	0.25		0.03
	6.8g	1	6.78	0.28	9.43	8.90	38.43	0.71	8.62	25.14	0.97	0.51		0.14
		2	3.56	1.3	13.8	12.68	46	0.03	0.3	20.12	0.28	0.54	0.56	0.85
	6.8h	1	1.04	5.34	12.38	27.15	25.23	0.81	0.62	26.40		0.04	0.31	0.41

Figure 6.8: Morphology and analysis of surface of the samples isothermally exposed at 650 ˚C: (a,b,c,d) coated with SM1 and (e,f,g,h) coated with SM2.

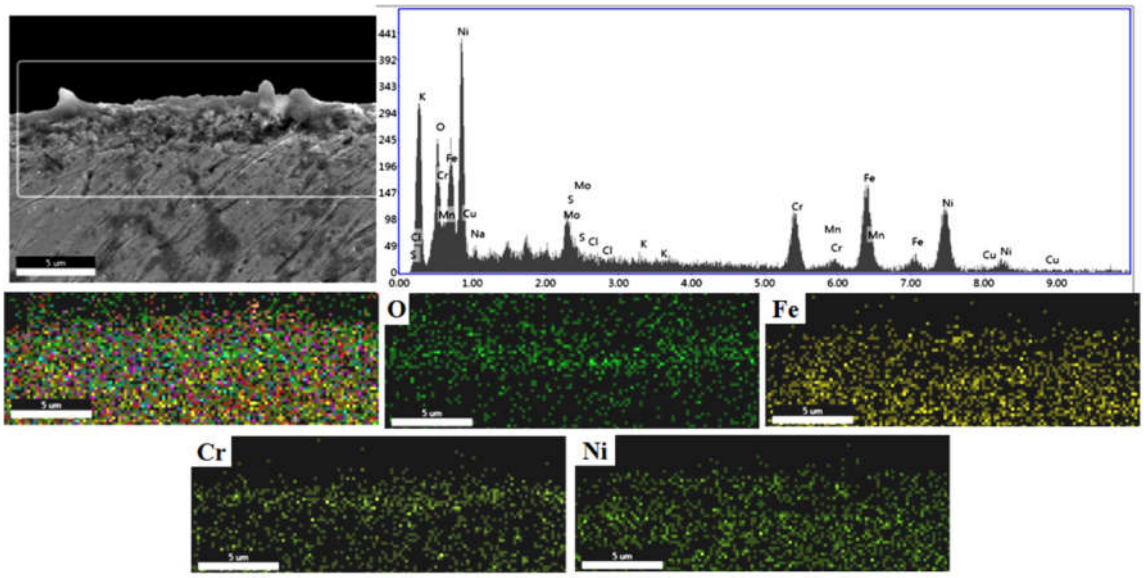

Figure 6.9: Cross sections of the SM1 coated sample isothermally exposed at 650 ˚C for 25 h, showing EDS peaks of different elements and mapping of O, Fe, Cr and Ni.

Cross section of the SM1 coated and SM2 coated samples exposed at 650 C for 100 h is shown in **Figure 6.11a**. It may be seen that there is internal damage below the interface of the scale and the substrate in a region of considerable width. The EDS peaks of the different elements are shown in **Figure 6.11b**. There is higher concentration of oxygen to large depth from the surface. Concentration of iron in the upper region of the scale is relatively less than below the surface concentration of chromium in the surface region is much less and is higher in the region below the surface, it again decreases and increases with depth from the surface. The concentration of nickel is less from surface to considerable depth and is higher in a narrow region. There is variation in the concentration of iron from surface towards interior.

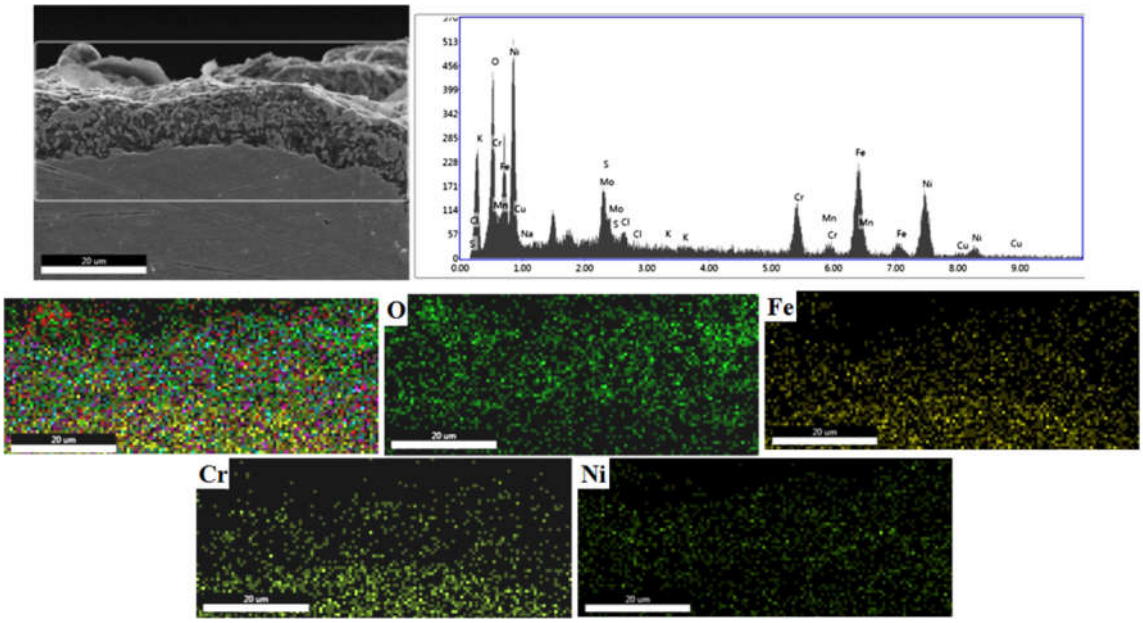

Figure 6.10: Cross sections of the SM2 coated sample isothermally exposed at 650 ˚C for 25 h, showing EDS peaks of different elements and mapping of O, Fe, Cr and Ni.

Cross section of the SM2 coated sample exposed at 650 ˚C for 100 h is shown in **Figure 6.12a**. The scale is quite uneven with voids and cracks. Also, there is internal damage to considerable depth. There is another region of internal damage below that of extensive damage. However, this region is relatively less damaged. The EDS peaks of different elements are shown in **Figure 6.12b**. There is high but non-uniform distribution of oxygen below the outermost surface and becomes more uniform with increase in depth. However, there is absence of oxygen in the lower region. There is variation in distribution of chromium, its concentration is less in the uppermost region of the scale, increases in the region below the upper one, again decreases and increases. There is low concentration of iron in the upper region of the scale.

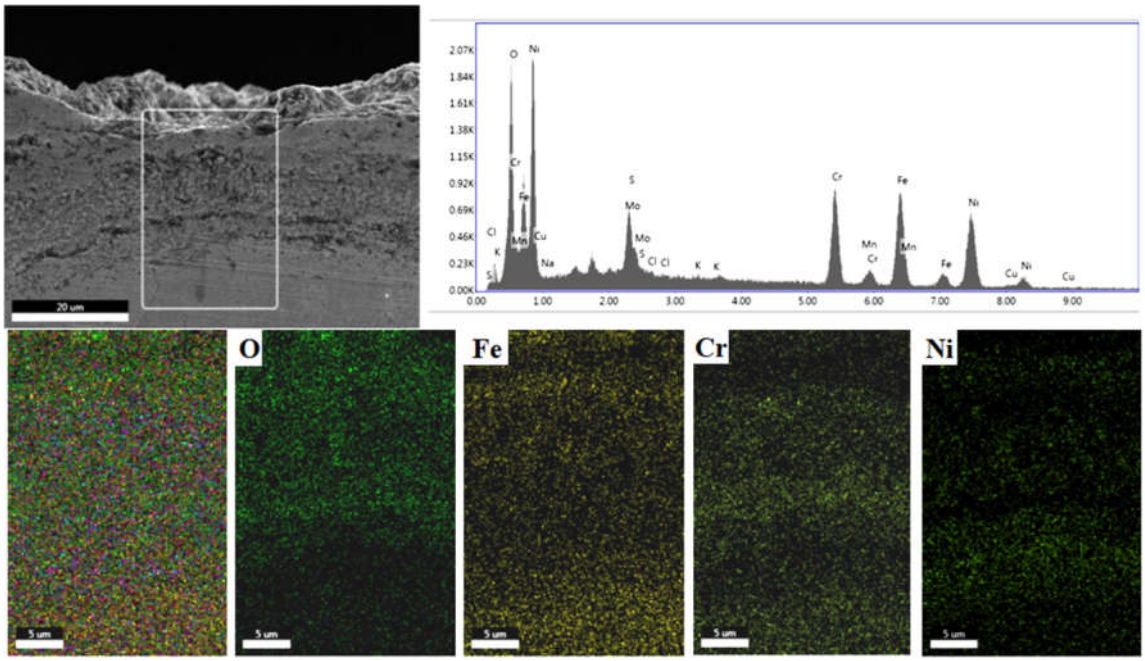

Figure 6.11: Cross sections of the SM1 coated sample isothermally exposed at 650 ˚C for 100 h, showing EDS peaks of different elements and mapping of O, Fe, Cr and Ni**.**

6.2.5 EPMA ANALYSIS

EPMA analysis of the specimens coated with SM2 isothermally exposed at 650 ˚C for 100 h, is shown in **Figure 6.13**. It may be seen that a non-uniform scale of varying thickness has formed and there is also internal oxidation in some regions. There is variation in concentration of oxygen in the scale. Iron concentration in the scale is low. There is enrichment of nickel at the top surface. There is discontinuity in concentration of chromium, it is seen to be high on the outermost surface, though it is non-uniform. Chromium is seen to be depleted from the region below the surface.

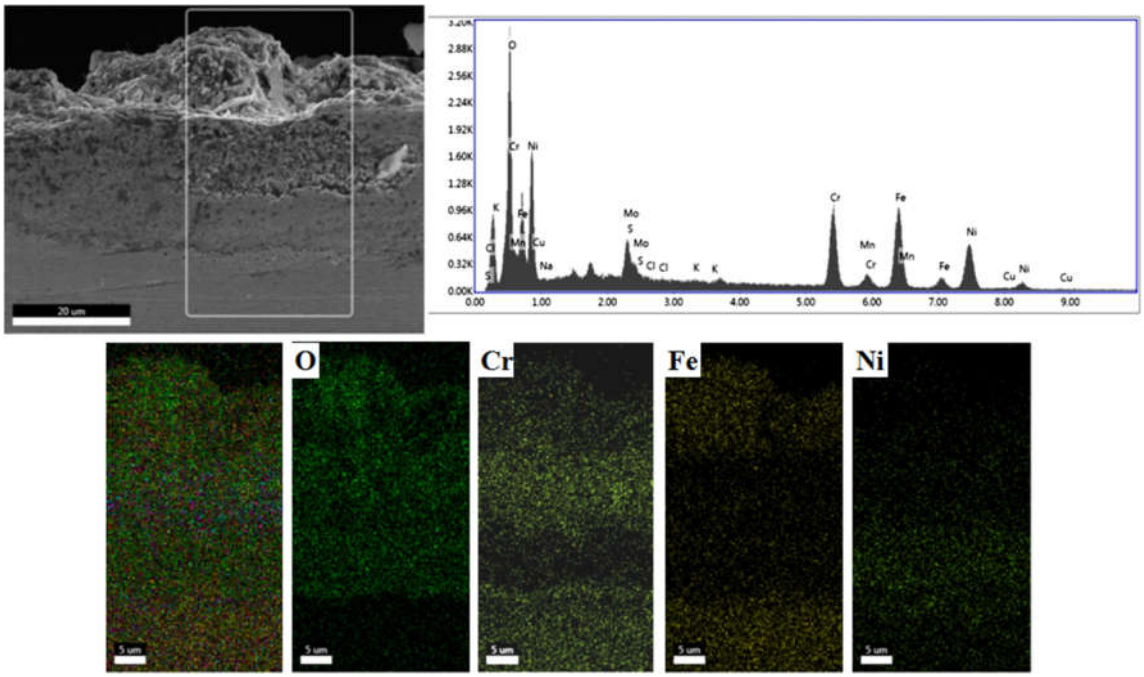

Figure 6.12: Cross sections of the SM2 coated sample isothermally exposed at 650 ˚C for 100 h, showing EDS peaks of different elements and mapping of O, Fe, Cr and Ni**.**

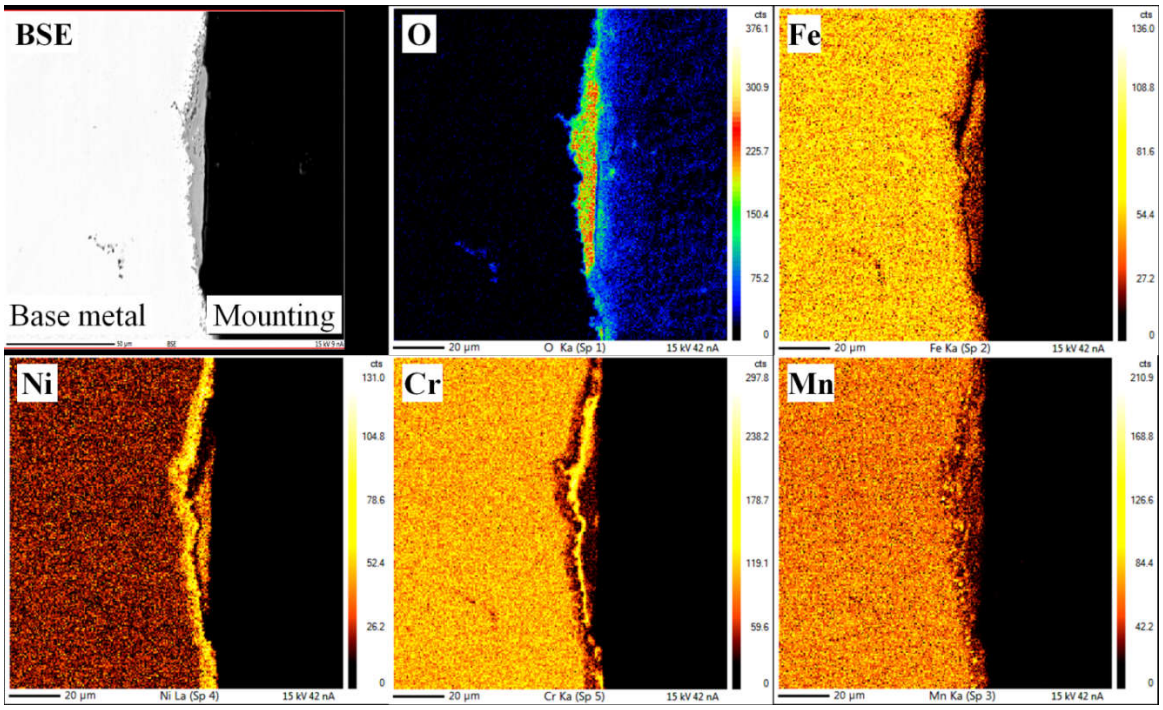

Figure 6.13: EPMA of cross section of the SM2 coated sample isothermally exposed at 650 ˚C for 100 h**.**

6.3. DISCUSSION

It is evident from the *ΔW vs t* plots in **Figure 6.1a and 6.2a** that weight gain in both the samples coated with SM1 as well as SM2 from isothermal exposure at 500 ˚C is almost comparable. It may be noted that the scale of ΔW in **Figure 6.2a** is much larger in respect of that in **Figure 6.1a** . However, at higher temperatures of exposure at 550, 600 and 650 ˚C weight gain (ΔW) is higher from the SM2 coating (**Figure 6.2a**). The disparity in ΔW of the SM1 and SM2 coated samples increases with rise in temperature from 550 to 650 ˚C. Thus, it is obvious that the damage resulting from the SM2 is more and it is due to higher proportion of the chloride containing salts than the sulphur containing salts in SM2 as compared with that in SM1. The process of hot corrosion resulting from the SM1 and SM2 coatings under the cyclic thermal exposure is discussed at length in Chapter 5. Even after cyclic oxidation the damage caused by SM2 coating is much higher than that resulting from the SM1 coating.

The comparison of the hot corrosion data of Chapter 5 (**Figure 5.2** and **Table 5.1**) with that of this chapter (**Figures 6.1** and **6.2, Table 6.1**) clearly shows that severity of hot corrosion under cyclic oxidation is more than that under isothermal oxidation from the SM1 and SM2 coatings. An examination of the phases formed under cyclic oxidation (Chapter 5, **Table 5.2**) with those formed under isothermal oxidation (Chapter 6, **Table 6.2**) shows that oxygen content in the coating formed under cyclic oxidation is more than that formed from isothermal oxidation at respective temperatures of exposure. The major difference between cyclic and isothermal hot corrosion may be considered to be associated with the stresses induced in the samples subjected to thermal cycles of heating and cooling. The other differences may be considered to be oxygen potential/partial pressure in the two

conditions. Naturally, oxygen potential is higher under cyclic exposure due to frequent opening of the furnace door. It is well established that damaging effect of the chlorides containing salts is due to breakdown of the protective chromia layer formed in the chromium containing alloys like Sanicro-25 and AISI 347. Chlorine reacts with chromium in the chromia layer and forms volatile $CrCl_3$. The formation of pores on the surface of these corroded samples is due to escape of such gaseous products through the oxide scale. It may be noted from the list of the reactions in **Table 5.5** in Chapter 5, that there is evolution of gaseous chlorine from the reactions involving oxygen. Liberation of gaseous chlorine and formation of chlorides like $FeCl_2/FeCl_3$ is highly damaging. It is quite evident from the EPMA analysis, of the hot corroded samples that the alloying elements responsible for formation of protective oxides get depleted due to rapid formation of damaging chlorides. In general, the scales formed from the hot corrosion are thick and porous due to volatilization of chlorides.

It may be seen from **Figures 6.1** and **6.2** that the rate of weight gain up to the initial 25 h was high and slowly decreased with the duration of exposure. It may be due to rapid formation of oxides of chromium and iron because of higher oxygen potential in the initial stage. It may be noted that in cyclic hot corrosion the rate of weight gain was significantly higher than that under isothermal exposure. This may be associated with the formation of protective oxide due to higher potential of oxygen in the furnace resulting from frequent opening of the furnace.

At 650 ˚C the rate of weight gain during the last stage of exposure from 75 to 100 h, was lowest. It may be outcome of spallation of scale and consequent formation of protective oxide over the large spalled region.

6.4. CONCLUSION

1. A near parabolic rate law is followed during corrosion of the SM1 and SM2 coated samples, over the temperature range from 500-650 ˚C.

2. The coating of the salt mixture SM2 is much more damaging than that of SM1 essentially due to damaging action of chloride ions than sulphide ions.

3. A wide range of surface morphology develops on the surface of the SM1 and SM2 coated samples, from isothermal exposures at 500-650 ˚C for varying duration of exposure.

4. The severity of damage resulting from the SM1 and SM2 coatings increases with temperature and duration of exposure.